THE JOURNAL OF BIOLOGICAL CHEMISTRY VOL. 289, NO. 32, pp. 22319–22332, August 8, 2014
Published in the U.S.A.

The Protease Inhibitor HAI-2, but Not HAI-1, Regulates Matriptase Activation and Shedding through Prostasin*

Received for publication, April 15, 2014, and in revised form, June 20, 2014 Published, JBC Papers in Press, June 24, 2014, DOI 10.1074/jbc.M114.574400

Stine Friis[‡§], Katiuchia Uzzun Sales[‡¶], Jeffrey Martin Schafer[‡‖], Lotte K. Vogel[§], Hiroaki Kataoka[**], and Thomas H. Bugge[‡1]

*From the [‡]Proteases and Tissue Remodeling Section, Oral and Pharyngeal Cancer Branch, and [¶]Clinical Research Core, NIDCR, National Institutes of Health, Bethesda, Maryland 20892, the [§]Department of Cellular and Molecular Medicine, Faculty of Health Science, University of Copenhagen, 2200 Copenhagen N, Denmark, the [‖]College of Medicine, The Ohio State University, Columbus, Ohio 43210, and the **Section of Oncopathology and Regenerative Biology, Department of Pathology, Faculty of Medicine, University of Miyazaki, 5200 Kihara, Kiyotake, Miyazaki 889-1692, Japan*

Background: Hepatocyte growth factor activator inhibitor (HAI)-1 and HAI-2 may regulate matriptase trafficking and activation.
Results: Ablation of endogenous HAI-2, but not HAI-1, causes loss of epithelial matriptase *in vivo* and *in vitro*, due to uncontrolled prostasin-dependent activation and shedding.
Conclusion: HAI-2, but not HAI-1, regulates matriptase cell surface expression level.
Significance: The study identifies HAI-2 as a principal regulator of prostasin-mediated matriptase activation.

The membrane-anchored serine proteases, matriptase and prostasin, and the membrane-anchored serine protease inhibitors, hepatocyte growth factor activator inhibitor (HAI)-1 and HAI-2, are critical effectors of epithelial development and postnatal epithelial homeostasis. Matriptase and prostasin form a reciprocal zymogen activation complex that results in the formation of active matriptase and prostasin that are targets for inhibition by HAI-1 and HAI-2. Conflicting data, however, have accumulated as to the existence of auxiliary functions for both HAI-1 and HAI-2 in regulating the intracellular trafficking and activation of matriptase. In this study, we, therefore, used genetically engineered mice to determine the effect of ablation of endogenous HAI-1 and endogenous HAI-2 on endogenous matriptase expression, subcellular localization, and activation in polarized intestinal epithelial cells. Whereas ablation of HAI-1 did not affect matriptase in epithelial cells of the small or large intestine, ablation of HAI-2 resulted in the loss of matriptase from both tissues. Gene silencing studies in intestinal Caco-2 cell monolayers revealed that this loss of cell-associated matriptase was mechanistically linked to accelerated activation and shedding of the protease caused by loss of prostasin regulation by HAI-2. Taken together, these data indicate that HAI-1 regulates the activity of activated matriptase, whereas HAI-2 has an essential role in regulating prostasin-dependent matriptase zymogen activation.

Epithelial development and homeostasis depends on a complex system of membrane-anchored trypsin-like serine proteases, including the type II transmembrane serine protease, matriptase, the glycophosphatidylinositol (GPI)[2]-anchored serine protease, prostasin, and the two Kunitz-type transmembrane serine protease inhibitors, hepatocyte growth factor activator inhibitor (HAI)-1 and HAI-2 (also known as Spint1 and Spint2, respectively) (reviewed in Ref. 1).

Matriptase is a 95-kDa type II transmembrane glycoprotein composed of a cytoplasmic N-terminal peptide, a signal anchor that functions as a single-pass transmembrane domain, a sea urchin sperm protein, enteropeptidase, agrin (SEA) domain, two complement C1r/s urchin embryonic growth factor and bone morphogenetic protein-1 (CUB) domains, four low-density lipoprotein receptor class A (LDLA) domains, and a trypsin-like serine protease domain (2–4). The FSEG^{149}-SVIA peptide bond in the SEA domain is spontaneously hydrolyzed during matriptase biosynthesis, but the newly formed N- and C-terminal halves of the protease are held together by strong non-covalent interactions within the SEA domain. This SEA domain auto-hydrolysis is a prerequisite for the subsequent activation site cleavage of matriptase after a conserved Arg^{614}, in the serine protease domain within the amino acid sequence RQAR^{614}-VVGG (5–7), which leads to the formation of the active protease. Activated matriptase subsequently is shed from the plasma membrane, facilitated by the formation of inhibitor complexes with HAI-1 (8, 9).

Prostasin is a 40-kDa GPI-anchored glycoprotein. It is synthesized as a zymogen that is converted to an active protease by a proteolytic cleavage after Arg^{44} within the amino acid sequence PQPR^{44}-ITGG (10–12).

HAI-1 and HAI-2 are closely related integral membrane proteins that are comprised of two extracellular Kunitz-type inhib-

* This work was supported by the NIDCR, National Institutes of Health, Intramural Research Program (to T. H. B.), by The Harboe Foundation, The Lundbeck Foundation, and The Foundation of 17.12.1981 (to S. F.), and by The Lundbeck Foundation (to L. V.).

[1] To whom correspondence should be addressed: Proteases and Tissue Remodeling Section, Oral and Pharyngeal Cancer Branch, NIDCR, National Institutes of Health, 30 Convent Drive, Room 320, Bethesda, MD 20892. Tel.: 301-435-1840; Fax: 301-402-0823; E-mail: thomas.bugge@nih.gov.

[2] The abbreviations used are: GPI, glycophosphatidylinositol; CUB, complement C1r/s urchin embryonic growth factor and bone morphogenetic protein-1; HAI, hepatocyte growth factor activator inhibitor; LDLA, low-density lipoprotein receptor class A; MANEC, motif at N-terminus with eight cysteines; PAR-2, protease-activated receptor-2; SEA, sea urchin sperm protein, enteropeptidase, agrin; SRE, serum response element.

itory domains that are followed by a C-terminal transmembrane domain. HAI-1 additionally contains a motif at N terminus with eight cysteines (MANEC) domain and a single LDLA domain located between the two Kunitz domains (13–15).

Activation of matriptase and prostasin in epithelial cells is accomplished by the formation of a reciprocal zymogen activation complex in which matriptase is activated by a non-catalytic allosteric interaction with the prostasin zymogen, and prostasin, in turn, is activated by a low intrinsic activity of the matriptase zymogen (16). Additional active matriptase may be generated by activation site cleavage of the matriptase zymogen by the newly activated prostasin, and additional active prostasin may be generated by activation site cleavage of the prostasin zymogen by the newly activated matriptase (16–18).

HAI-1 was first purified from milk as a soluble protein that formed a stable complex with cell surface-shed activated matriptase, immediately suggesting a role of HAI-1 in regulating the membrane-anchored serine protease (19). Indeed, subsequent studies showed that stable protease-inhibitor protein complexes are formed between HAI-1 and activated matriptase in *ex vivo* systems with purified components, in epithelial cell cultures, and in organotypic cultures (20–22). HAI-1 also was found to form stable inhibitor complexes with prostasin, suggesting a dual function in regulating the matriptase-prostasin system (20, 22, 23). Compatible with these biochemical observations, subsequent genetic epistasis analysis placed HAI-1 downstream from both matriptase and prostasin during development (24–26). In fact, HAI-1 becomes dispensable for development and long-term survival of mice with low levels of either active matriptase or prostasin (27, 28), suggesting that a principal role of the inhibitor is to restrict the activity of the matriptase-prostasin system. More recently, a similar role in regulating the matriptase-prostasin system has been ascribed to HAI-2, based on the ability of soluble recombinant HAI-2 to form high affinity inhibitor complexes with soluble recombinant matriptase, and on the genetic rescue of developmental defects in HAI-2-deficient animals that can be achieved by either loss of expression or by low-level expression of matriptase or prostasin (20, 25, 28).

In addition to the canonical role of HAI-1 and HAI-2 in restricting the activity of matriptase subsequent to its activation, both inhibitors also have been proposed to have unique functions in regulating the intracellular trafficking and activation of matriptase. Thus, HAI-1 is reported to interact with the matriptase zymogen already within the biosynthetic pathway to prevent its premature activation, to facilitate its transport to the cell surface, and even to induce its activation once located on the plasma membrane (6, 29–32). Likewise, HAI-2 was recently suggested to be critical for the retention of active matriptase on the plasma membrane (33). A potentially confounding factor in these studies, however, is the frequent reliance on cell-based overexpression systems to dissect the mechanistic interactions of matriptase with HAI-1 and HAI-2. Moreover, discrepancies have been reported as to the necessity of HAI-1 for proper expression of matriptase, even within the same cell-based model system (33–35).

Cognizant of the considerable knowledge gaps regarding these putative non-traditional roles of HAI-1 and HAI-2 in matriptase function, herein we used a novel approach to analyze the functional relationship of the two inhibitors with the matriptase-prostasin system. Rather than relying on overexpression models, we used gene targeting and gene silencing to determine the effect of ablating endogenous HAI-1 and HAI-2 on endogenous matriptase cell surface localization, activation, and shedding in mouse intestinal epithelia and in intestinal epithelial cell monolayers. We find that loss of HAI-1 does not affect cell surface localization or abundance of matriptase in polarized epithelium of either the small intestine or the colon. In contrast, loss of HAI-2 causes a dramatic decrease in cell surface expression of matriptase in intestinal epithelia, which is mechanistically linked to increased prostasin-mediated activation and shedding.

MATERIALS AND METHODS

Mouse Strains and Tamoxifen Gavage—All experiments were performed in an Association for Assessment and Accreditation of Laboratory Animal Care International-accredited vivarium following Standard Operating Procedures. The studies were approved by the NIDCR Institutional Animal Care and Use Committee. All studies were littermate controlled. $Spint^{LoxP/LoxP}$, $Spint1^{-/-}$;$Prss8^{fr/fr}$, $Spint2^{-/-}$;$Prss8^{fr/fr}$, $St14^{-/-}$, $Villin\text{-}Cre^{+/0}$;$St14^{loxP/loxP}$ mice have been described previously (28, 36–38). Heterozygous *Spint1* mice ($Spint1^{+/-}$) were bred with mice harboring a tamoxifen-inducible Cre recombinase under the control of the ubiquitously expressed β-actin promoter ($\beta\text{-}actin\text{-}Cre^{+/0}$), obtained from The Jackson Laboratory (Bar Harbor, Maine). The $Spint1^{+/-}$ offspring carrying a β-actin-Cre recombinase allele ($\beta\text{-}actin\text{-}Cre^{+/0}$;$Spint1^{+/-}$) were bred to $Spint^{LoxP/LoxP}$ mice to generate $\beta\text{-}actin\text{-}Cre^{+/0}$;$Spint^{LoxP/-}$ mice in a mixed 129/FVB/N/C57BL6/J background. At 6 weeks of age, the $\beta\text{-}actin\text{-}Cre^{+/0}$;$Spint1^{LoxP/-}$ mice and littermate controls were gavaged with 10 μg tamoxifen (dissolved in vegetable oil)/g body weight for 5 consecutive days followed by euthanasia and tissue collection 2 days later.

Protein Extraction from Mouse Tissue—The tissues were dissected, snap frozen on dry ice, and stored at −80 °C until homogenization. The tissues were homogenized in ice-cold lysis buffer containing 1% Triton X-100, 0.5% sodium-deoxycholate in phosphate-buffered saline (PBS) plus Proteinase Inhibitor Mixture (Sigma) and incubated on ice for 10 min. The lysates were centrifuged at 20,000 × *g* for 20 min at 4 °C to remove the tissue debris, and the supernatant was used for further analysis. The protein concentration was measured with standard BCA assay (Pierce).

Cell Culture—HEK293 cells were grown in Dulbecco's modified Eagles medium (DMEM) supplemented with 2 mM l-glutamine, 10% fetal bovine serum, 100 units/ml penicillin, and 100 μg/ml streptomycin. Caco-2 cells (ATCC, Manassas, VA) were grown in DMEM supplemented with 2 mM L-glutamine, 20% fetal bovine serum, 1× nonessential amino acids, 100 units/ml penicillin, and 100 μg/ml streptomycin (Invitrogen) at 37 °C in an atmosphere of 5% CO_2. For all experiments, 2×10^6 cells were seeded into 0.4 μm pore-size, 24 mm Transwell® filter chamber plates (Corning, Corning, NY) that allow sepa-

rate access to the apical and basolateral plasma membrane. The tightness of filter-grown cells was assayed by filling the inner chamber to the brim with cell culture media and allowing it to equilibrate overnight. The cell culture medium was changed every other day.

Transfection of siRNA in Caco-2 Cells and Immunoprecipitation—Subconfluent Caco-2 cells (10^6 cells/transfection) were transfected in suspension with siRNA (SPINT2; HSS116435, HSS116436, HSS173811, PRSS8; HSS108633, HSS108631, controls; 46–2000, 46–2001, 46–2002 (Invitrogen)) using Dharmafect1 (Thermo Scientific, Hudson, NH), following the manufacturer's instructions. For the siRNA, 3.3 μl of 20 μm RNA stock and 7 μl of transfection agent in a final volume of 2 ml of serum-free medium were used. The transfected Caco-2 cells were seeded on 6-well Transwell filters. The medium was changed 12–24 h after transfection, and 72 h post-transfection, the cells were lysed in lysis buffer (1% Triton X-100, 0.5% sodium deoxycholate in PBS) plus Proteinase Inhibitor Mixture (Sigma) and were spun for 20 min at 20,000 $\times$ *g* at 4 °C. For immunoprecipitation the inhibitor mixture was excluded. Gammabind G-Sepharose (GE Healthcare, Upsala, Sweden) was prepared as instructed by the manufacturer. The lysates were pre-cleared with 40 μl of Sepharose for 30 min at 4 °C with end-over-end rotation where after the samples were spun 2 min at 1,500 $\times$ *g* and the supernatant was transferred to a new tube containing 75 μl of Sepharose and 20 μg of polyclonal goat anti-human HAI-2 antibody (R&D Systems, AF1106). The immunoprecipitation was incubated for 5 h at 4 °C with end-over-end rotation. After incubation the samples were spun at 2,000 $\times$ *g* at 4 °C to precipitate the affinity gel. The gel was subsequently washed three times with wash buffer I (25 mM Tris/HCl, pH 7.8, 500 mM NaCl, and 0.5% Triton X-100) followed by four washes with wash buffer II (10 mM Tris/HCl, pH 7.8, and 150 mM NaCl). The precipitated proteins were eluted by boiling in 2$\times$ sample buffer for 7 min and analyzed by Western blot as described above.

Immunofluorescence Analysis of Mouse Intestine—Intestinal samples from mice were fixed in 4% paraformaldehyde in PBS for 24 h, embedded into paraffin, and sectioned. Tissue sections were cleared with xylene-substitute (Safe Clear, Fisher Scientific), rehydrated in a graded series of alcohols, and boiled in Reduced pH Retrieval Buffer (Bethyl, Montgomery, TX) for 20 min for antigen retrieval. The sections were blocked for 1 h in PBS containing 10% horse serum and incubated at 4 °C overnight with sheep anti-human matriptase (AF3946, R&D Systems, Minneapolis, MN) or goat anti-mouse HAI-1 (AF1141, R&D Systems) and rabbit anti-mouse E-cadherin (Zymed Laboratories Inc., Invitrogen, Carlsbad, CA). The slides were washed 3 times in PBS and incubated at room temperature for 45 min with secondary antibodies, Alexa fluor 594-labeled donkey anti-sheep (Invitrogen) and FITC-labeled goat anti-rabbit (Zymed Laboratories Inc.). The tissue sections were washed three times for 5 min with PBS and mounted with VectaShield Hard Set Mounting Medium (Vector Laboratories Inc., Burlingame, CA). The samples were subjected to laser scanning confocal microscopy using the Leica TCS SP2 system and Zeiss LS700 system.

Immunofluorescence Analysis of Caco-2 Cells—Caco-2 cells grown on Transwell filters were fixed for 20 min in 4% paraformaldehyde in PBS (Z-fix, Anatech, Battle Creek, MI) at room temperature. The following procedures were performed on ice unless otherwise specified. Cells were permeabilized with 0.05% Triton X-100 in PBS for 20 min. Unspecific staining was blocked with PBS containing 5% BSA (PBS/BSA) for 1 h. Cells were incubated with primary antibody diluted in PBS/BSA overnight at 4 °C. The antibodies used for immunofluorescence were mouse monoclonal anti-human matriptase, M32, (39), and polyclonal rabbit anti-human occludin (71–1500, Zymed Laboratories Inc.). The next day the cells were washed three times in PBS, followed by incubation with relevant Alexa Fluor-conjugated secondary antibodies (Invitrogen) for 1 h. The cells were finally washed 3$\times$ in PBS and mounted with Vectashield Hard Set Mounting Medium (Vector Laboratories Inc.) and subjected to laser scanning confocal microscopy using the Leica TCS SP2 system and Zeiss LS700 system.

Western Blotting—Samples were mixed with 4$\times$ SDS sample buffer (NuPAGE, Invitrogen) containing 7% β-mercaptoethanol and boiled for 10 min, unless otherwise indicated. The proteins were separated on 4–12% BisTris NuPage gels and transferred to 0.2-μm pore size PVDF membranes (Invitrogen). The membranes were blocked with 5% nonfat dry milk in Tris-buffered saline (TBS) containing 0.05% Tween 20 (TBS-T) for 1 h at room temperature. The individual PVDF membranes were probed with primary antibodies diluted in 1% nonfat dry milk in TBS-T overnight at 4 °C. Antibodies used for mouse lysates were sheep anti-human matriptase (AF3946, R&D Systems), polyclonal goat anti-mouse HAI-1 (AF1141, R&D Systems), polyclonal goat anti-mouse HAI-2 (AF1107, R&D Systems), and mouse anti-human prostasin (catalogue no. 612173, BD Transduction Laboratories, San Jose, CA). Before applying the goat anti-mouse HAI-2 antibody to the PVDF membrane for overnight probing, the antibody was pre-absorbed with 10 μg of protein from HAI-2 knock-out lysate for 30 min at 4 °C in 1% nonfat dry milk/PBS-T. Antibodies used for Caco-2 cell lysates were sheep anti-human matriptase (AF3946, R&D Systems), mouse anti-human matriptase monoclonal antibody M69 (39), goat anti-human HAI-1 (AF1048, R&D Systems), polyclonal rabbit anti-human SPINT2 (HPA011101, Sigma) and mouse anti-human prostasin (catalogue no. 612173, BD Transduction Laboratories). For both mouse and cell lysates α-tubulin was used as a loading control (Cell Signaling, Beverly, MA, 9099S). The next day, the membranes were washed three times for 5 min each in TBS-T and incubated for 1 h with alkaline phosphatase-conjugated secondary antibodies (Thermo Scientific). After three 5-min washes with TBS-T, the signal was developed using nitro blue tetrazolium/5-bromo-4-chloro-3-indolyl phosphate solution (Pierce).

RT-PCR on Mouse Tissue—Intestines were snap-frozen in liquid nitrogen and ground to a fine powder with a mortar and pestle. Total RNA was prepared by extraction in Trizol reagent (Invitrogen), as recommended by the manufacturer. Reverse transcription and PCR amplification were performed using the RETROscript™ Kit (Ambion Inc., Austin, TX), as recommended by the manufacturer. First strand cDNA synthesis was performed using an Oligo dT primer. The following primer pairs were used for qPCR: *St14*; 5′-AGATCTTTCTGGATGCGTATGAGA-3′ and 5′-GGACTTCATTGTACAGCA-

GCTTCA-3′. The annealing temperature for these primer sets was 58 °C. Expression levels were normalized to 18 S in each sample; 5′-GAACTGCGAATGGCTCATTAAA-3′ and 5′-CCACAGTTATCCAAGTAGGAGAGGA-3′.

PAR-2 Activation Assay—The assay was performed essentially as described (16). HEK293 cells (250,000 cells/well) were plated in 24-well poly-L-lysine-coated plates and grown for 24 h. Cells were co-transfected with pSRE-firefly luciferase (50 ng) (40), pRL-*Renilla* luciferase (20 ng), pcDNA3.1 containing a full-length human protease-activated receptor (PAR)-2 cDNA (100 ng) (Missouri S&T cDNA Resource Center), pcDNA3.1 containing human matriptase (100 ng), pcDNA3.1 containing human HAI-1 (100 ng), pIRES2-EGFP human prostasin (100 ng) (18), pBig-HAI-2HA (100 ng) and doxycycline inducible rtTA2S-M2 Tet-transactivator, as indicated in the individual experiments (41). Lipofectamine (Invitrogen) was used as the transfection agent according to the manufacturer's instructions. The pBig-HAI-2HA plasmid was generated by inserting the full-length murine Spint2 cDNA (NP_001076017.1) with a synthetic DNA sequence encoding a C-terminal human influenza hemagglutinin (HA)-Tag (YPYDVPDYA) inserted just prior to the stop codon into a unique NotI site of the pBig transgene expression vector containing a Tet responsive element (TRE) (Clonetech, Mountain View, CA). The pSRE-firefly luciferase is a luciferase reporter gene under the control of a multimerized serum-response element. The transfection medium was changed after 18 h, and 48 h after transfection, the cells were serum-starved overnight while induced with Doxycycline (1 μg/ml). Cells were lysed, and luciferase activity was determined using the Dual-Luciferase assay kit (Promega) according to the manufacturer's instructions. Luminescence was measured using a Wallac Victor2 1420 multilabel counter (PerkinElmer Life Sciences), and the serum-response element activity was determined as the ratio of firefly luciferase to *Renilla* luciferase light units.

Transfection of HAI-2 HA in HEK293T Cells and Immunoprecipitation—For the human pcDNA3.1 HAI-2 construct the HA-tag was positioned between amino acid (AA) 30 and 31 to preserve the N-terminal signal peptide (AA 1–27). The HA-tag was inserted in the HAI-2 pcDNA3.1 vector encoding full-length human HAI-2 cDNA (inserted with EcoRI) with the use of QuickChange site-directed mutagenesis kit according to the protocol provided by the manufacturer (Stratagene, La Jolla, CA). The primers contained the HA-tag sequence (lowercase letters): HAI-2HA forward, 5′-tatccttatgacgtgcctgactatgccCGCAGCATCCACGACTTC-3′, HAI-2HA reverse, 5′-CTGGCGGCCGACCGAGAAtatccttatgacgtgcctgactatgcc-3′. HEK293T cells were grown to 95% confluency on poly-L-lysine-coated plates before they were co-transfected with human HAI-2 cDNA in the pcDNA3.1 vector (either with or without the HA tag), full-length human matriptase in the pcDNA3.1 vector and full-length human prostasin cDNA in the pIRES-EGFP vector. Lipofectamine (Invitrogen) was used according to the manufacturer's instructions, transfecting a total of 4 μg DNA in a 6 well format. The cells were lysed 48 h post-transfection, and the lysates were spun at 20,000 × *g* at 4 °C for 20 min. A fraction of the supernatant was used for Western blot and the remaining was used for immunoprecipitation. The EZview Red anti-HA affinity gel (Sigma) was prepared according to the manufacturer's instructions. Each sample was added to 50 μl affinity gel and incubated end-over-end for 5 h at 4 °C. After incubation the samples were spun at 2,000 × *g* at 4 °C to precipitate the affinity gel. The gel was subsequently washed three times with wash buffer I (25 mM Tris/HCl, pH 7.8, 500 mM NaCl, and 0.5% Triton X-100) followed by four washes with wash buffer II (10 mM Tris/HCl, pH 7.8, and 150 mM NaCl). The precipitated proteins were analyzed by Western blot as described above.

RESULTS

Loss of Endogenous HAI-1 Does Not Affect Expression or Subcellular Localization of Endogenous Matriptase in Intestinal Epithelium—We used Western blotting and immunofluorescence to directly determine the protein expression levels and the subcellular localization of endogenous matriptase in intestinal epithelia in the absence of endogenous HAI-1 and HAI-2. We chose to study mouse intestinal epithelium because matriptase, prostasin, HAI-1, and HAI-2 are all expressed in this tissue, because the matriptase-prostasin system is critical for intestinal epithelial homeostasis, and because matriptase is expressed at high levels and displays a distinct basolateral localization at steady state (20, 42–44). Since the validity of our experiments was critically dependent on the ability to specifically detect membrane-localized matriptase in intestinal epithelial cells, we first performed matriptase immunofluorescence analysis on wild type and matriptase-deficient intestines (Fig. 1). Immunofluorescence staining of wild type intestine using the polyclonal sheep anti-matriptase antibody, AF3946, resulted in strong staining of the basolateral membranes of epithelial cells of both the small intestine (Fig. 1, *A–C*) and the large intestine (Fig. 1, *G–I*), which co-localized with the cell-cell adhesion protein E-cadherin. This staining was absent in matriptase-deficient epithelial cells from both small (Fig. 1, *D–F*) and large (Fig. 1, *J–L*) intestine, demonstrating that cell surface matriptase can be specifically detected in both tissues using this antibody, and that changes in the abundance and distribution of matriptase in intestinal epithelial cells can be readily determined.

We next used two separate approaches to directly determine the effect of ablation of endogenous HAI-1 from intestinal epithelial cells on the expression and subcellular localization of endogenous matriptase. First, we used young adult mice carrying a floxed and a null *Spint1* allele and also carrying a tamoxifen-inducible Cre recombinase gene under the control of a β-actin promoter ($Spint1^{LoxP/-}$;β-*actin-Cre-ERtm*$^{+/0}$ mice). Littermate $Spint1^{LoxP/+}$ mice were used as controls. These mice were subjected to daily tamoxifen treatments over a period of 5 days to ablate HAI-1 from intestinal tissues. Intestinal tissue was analyzed for matriptase expression and subcellular localization 2 days after the final tamoxifen treatment to prevent the demise of epithelial tissue architecture associated with long-term HAI-1 ablation (36) from confounding the data interpretation. HAI-1 was successfully ablated from the intestine by the tamoxifen treatment, as shown by Western blotting (example in Fig. 2*A*, *top panel*, compare *lanes 1–3* to *lanes 4* and *5*) and immunofluorescence (*insets* in Fig. 2, *G* and *O*, compare with *insets* in *C* and *K*, respectively) using HAI-1 antibodies. Inter-

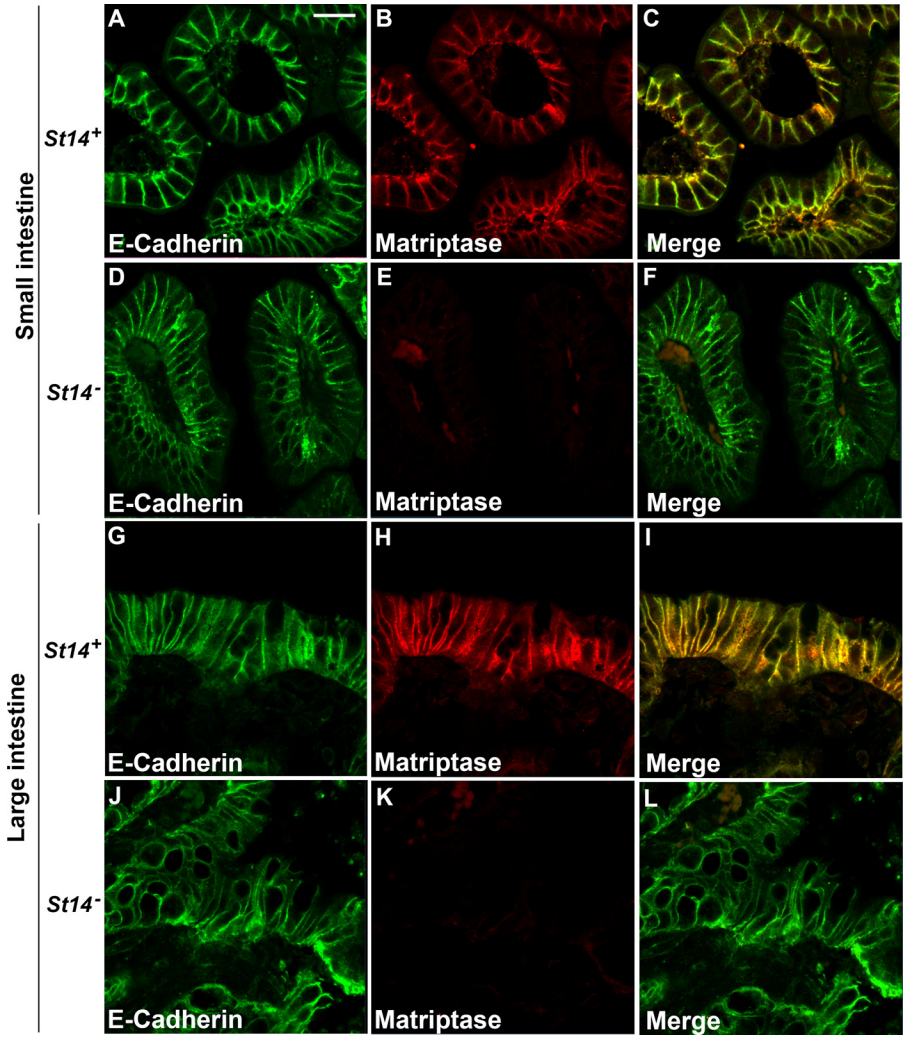

FIGURE 1. **Specific detection of endogenous matriptase in intestinal epithelium.** The distribution of E-cadherin (*A*, *D*, *G*, *J*) and matriptase (*B*, *E*, *H*, and *K*) in small intestine (*A–F*) and large intestine (*G–L*) of matriptase-sufficient (*Villin-Cre*$^{+/0}$; *St14*$^{fl/+}$) (*A–C*, *G–I*) and intestinal matriptase-deficient (*Villin-Cre*$^{+/0}$; *St14*$^{fl/-}$) mice (*D–F*, *J–L*) demonstrating that the antibody AF3946 is matriptase specific. Matriptase and E-cadherin are merged in *C*, *F*, *I*, and *L*. *Scale bar*, 20 μm. The data are representative of two similar experiments.

estingly, the matriptase protein level in the intestine was unaffected by the loss of HAI-1, as shown by similar levels of matriptase in protein extracts from intestinal tissues from HAI-1-sufficient and HAI-1-deficient mice analyzed by reducing SDS-PAGE and Western blotting using a matriptase antibody that recognizes an epitope located within the serine protease domain (example in Fig. 2*A*, *second panel from top*, *lanes 1–3*, compare with *lanes 4* and *5*). Furthermore, the subcellular localization of matriptase was unaffected by the depletion of HAI-1 in epithelial cells of both the small (example in Fig. 2, *F–I*, compare with Fig. 2, *B–E*) and in large (Fig. 2, *N–Q*, compare with *J–M*) intestine, as analyzed by immunofluorescence and confocal microscopy. This absence of an effect of HAI-1 expression on matriptase levels and subcellular localization could not be explained by a compensatory up-regulation of HAI-2, as the level of expression of HAI-2 was unaffected by the presence or absence of HAI-1 (example in Fig. 2*A*, *second panel from bottom*, compare *lanes 1–3* to *lanes 4* and *5*). The predicted molecular mass of HAI-2 is 28 kDa but splice variants A and B have been reported as well as glycosylation of the protein, rendering two major bands around 32 and 28 kDa (14, 45).

HAI-1 is expressed in a high molar excess to matriptase in most epithelial cells (46). A potential caveat of the above experiment, therefore, was that residual HAI-1 could be expressed at levels that eluded detection by Western blot or by immunofluorescence, but were sufficient to allow for appropriate transport to the epithelial cell surface. To examine this possibility, our second approach was to investigate matriptase expression and subcellular localization in intestinal tissues of mice in which complete HAI-1 deficiency was compensated by a hypomorphic mutation in the prostasin gene (*Spint1*$^{-/-}$;*Prss8*$^{fr/fr}$ mice) using HAI-1-sufficient prostasin hypomorphic (*Spint1*$^{+/+}$; *Prss8*$^{fr/fr}$) littermates as controls (28, 47). Again, intestinal matriptase protein expression levels were unaffected by the absence of HAI-1, as determined by Western blot (example in Fig. 3*A*, *second panel from top*, *lanes 1–3*, compare with *lanes 4–6*). Likewise, the subcellular distribution of matriptase again was unaffected by the absence of HAI-1 in epithelial cells of both the small (example in Fig. 3, *F–I*, compare with *B–E*) and the large (example in Fig. 3, *N–Q*, compare with *J–M*) intestine. As above, the absence of an effect of HAI-1 ablation on matriptase levels and subcellular localization could not be explained

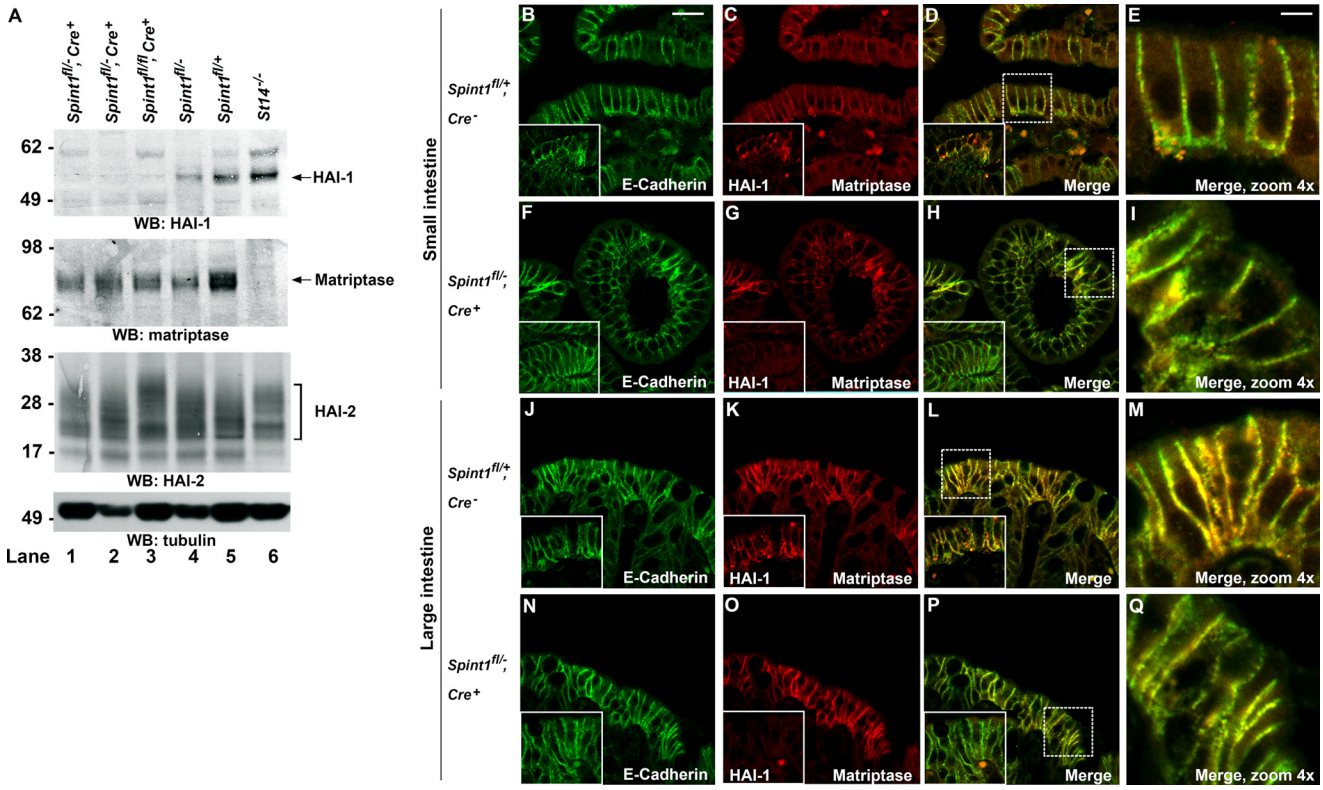

FIGURE 2. **Loss of HAI-1 does not affect the abundance or subcellular distribution of matriptase in epithelium of the large and small intestine.** *A*, lysates of intestines from 6-week-old HAI-1-ablated mice (*Spint1*$^{fl/-}$; *Cre*$^{+}$, *lanes 1–3*) and littermate controls expressing HAI-1 (*Spint1*$^{fl/-}$ or *Spint1*$^{fl/+}$; *Cre*$^{-}$, *lanes 4* and *5*). Matriptase-deficient intestine (*Villin-Cre*$^{+/0}$; *St14*$^{fl/-}$) was included as a control for antibody specificity in *lane 6*. The lysates were boiled, reduced, and analyzed by Western blot using antibodies against HAI-1 (*top panel*), matriptase (*second panel from top*), and HAI-2 (*second panel from bottom*). Tubulin was used as a loading control (*bottom panel*). The specific proteins are indicated on the *right*, and molecular markers are indicated on the *left* (kDa). The data are representative of three similar experiments. The distribution of matriptase (*C*, *G*, *K*, and *O*) and E-cadherin (*B*, *F*, *J*, *N*) in small intestine (*B–I*) and large intestine (*J–Q*) in mice expressing HAI-1 (*B–E* and *J–M*) and HAI-1-depleted mice (*F–I* and *N–Q*). Matriptase and E-cadherin are merged in *D*, *H*, *L*, and *P* with enlargements of indicated area (shown with *white dotted line*) in *E*, *I*, *M*, and *Q*, respectively. HAI-1 staining of the same tissue is represented in the inset in C, G, K and O together with E-cadherin (*inset*, *B*, *F*, *J*, and *N*). The merge of HAI-1 and E-cadherin is shown in the *inset* in *D*, *H*, *L*, and *P*. Scale bar in *B*, 20 μm, representative for *B–D*, *F–H*, *J–L*, *N–P*. Scale bar in *E*, 5 μm, representative for *E*, *I*, *M*, and *Q*. The data are representative of three similar experiments.

by a compensatory up-regulation of HAI-2, as the level of expression of HAI-2 was unaffected by the presence or absence of HAI-1 (example in Fig. 3*A*, *third panel from top*, compare *lanes 1–3* to *lanes 4–6*). Also, no significant alteration in prostasin level was observed in the absence of HAI-1 (example in Fig. 3*A*, *second panel from bottom*, compare *lanes 1–3* to *4–6*). Taken together, the above studies demonstrate that the level of expression and the subcellular localization of endogenous matriptase in intestinal cells of the small and large intestine are unaffected by the presence or absence of endogenous HAI-1.

Loss of Endogenous HAI-2 Reduces Expression of Endogenous Matriptase in Intestinal Epithelial Cells—We next examined the effect of endogenous HAI-2 deficiency on the expression and subcellular localization of endogenous matriptase in intestinal epithelium. For this purpose, we used mice in which the embryonic lethality caused by complete HAI-2 deficiency is bypassed by the hypomorphic prostasin gene mutation (*Spint2*$^{-/-}$;*Prss8*$^{fr/fr}$) (28, 47) and we used HAI-2-sufficient prostasin hypomorphic (*Spint2*$^{+/+}$;*Prss8*$^{fr/fr}$) littermates as controls (example in Fig. 4*A*, *top panel*, compare *lanes 1* and *2* with *3* and *4*). Interestingly, the level of expression of endogenous intestinal epithelial matriptase was markedly decreased by the absence of HAI-2, as determined by reducing SDS-PAGE and Western blotting (example in Fig. 4*A*, *second panel from top*, compare *lanes 1* and *2* with *lanes 3* and *4*). As was the case for HAI-2, no compensatory increase in HAI-1 expression in HAI-2-deficient intestines was observed, although considerable genotype-independent fluctuations in HAI-1 expression levels were observed (example in Fig. 4*A*, *third panel from top*, compare *lanes 1* and *2* with *lanes 3* and *4*). No significant increase of prostasin was observed (Fig. 4*A*, *second panel from bottom*) when compared with the level of tubulin that was used as a loading control (Fig. 4*A*, *bottom panel*). To determine if the decrease in the expression of matriptase protein in HAI-2-deficient intestines was due to regulation at the level of transcription or mRNA processing, we compared intestinal *St14* mRNA in *Spint2*$^{-/-}$, *Spint2*$^{+/-}$, and *Spint2*$^{+/+}$ littermates (Fig. 4*B*). This analysis showed that *St14* mRNA levels were not different in mice of the three genotypes, suggesting that endogenous HAI-2 regulates endogenous matriptase expression at the translational or post-translational level. Using immunofluorescence, we next analyzed the subcellular localization of matriptase in HAI-2-deficient intestinal epithelium. In agreement with the reduced abundance of matriptase revealed by Western blot, matriptase could not be detected on the basolateral membrane of HAI-2-deficient intestinal epithelial cells, with residual low matriptase expression found only in intracellular structures of both the small (example in Fig. 4, *G–J*, compare with

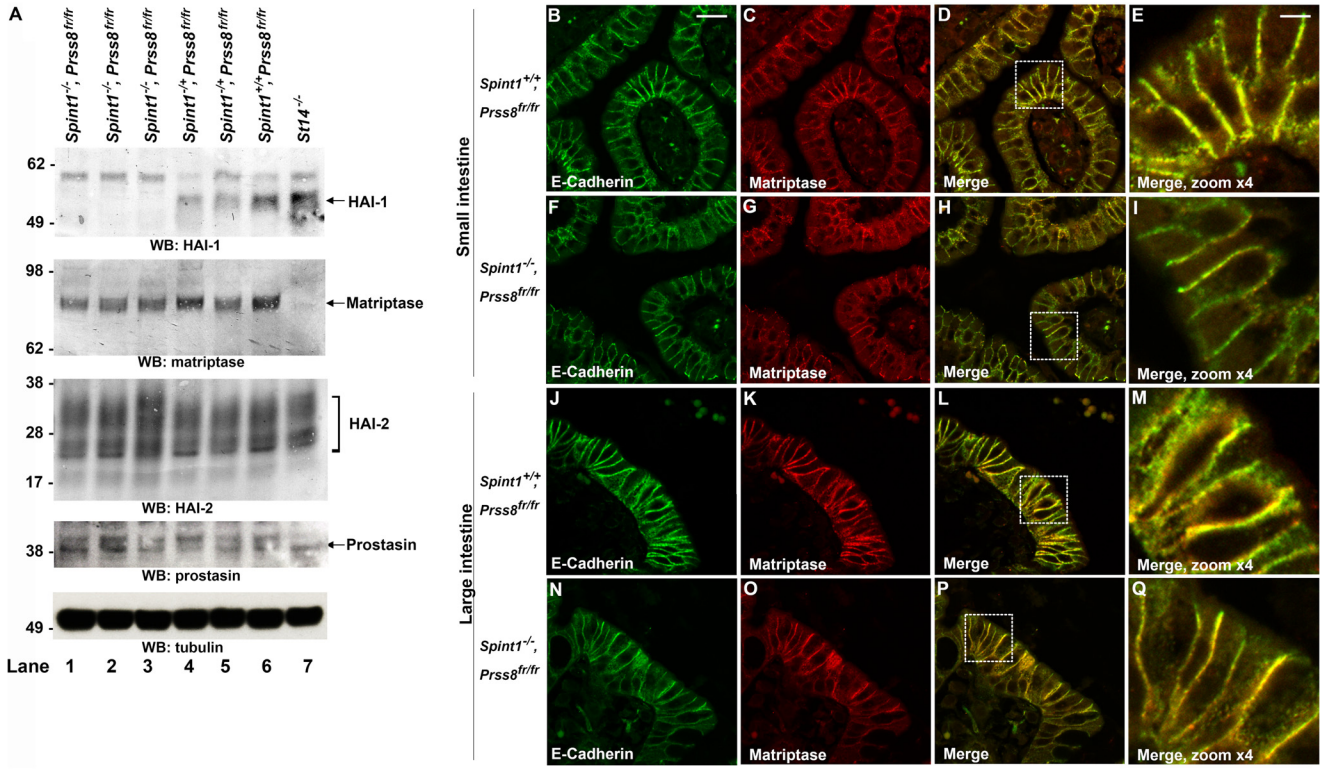

FIGURE 3. **Normal levels and distribution of matriptase in the intestine of HAI-1 knock-out mice in the prostasin hypomorphic background fr/fr.** *A*, lysates of intestines from 1-year-old HAI-1 knock-out mice (*Spint1*$^{-/-}$*; Prss8*$^{fr/fr}$, *lanes 1–3*) and littermate controls expressing HAI-1 (*Spint1*$^{+/-}$ *or Spint1*$^{+/+}$*; Prss8*$^{fr/fr}$, *lanes 4–6*). Matriptase-deficient (*Villin-Cre*$^{+/0}$, *St14*$^{fl/-}$) intestine was included as control (*lane 7*). The lysates were boiled, reduced, and analyzed by Western blotting using antibodies against HAI-1 (*top panel*), matriptase (*second panel from top*), HAI-2 (*third panel from top*) and prostasin (*second panel from bottom*). Tubulin was used as loading control (*bottom panel*). The specific proteins are indicated on the *right* and molecular markers are indicated on the *left* (kDa). The data are representative of three similar experiments. The distribution of matriptase (*C*, *G*, *K*, and *O*) and E-cadherin (*B*, *F*, *J*, and *N*) in small intestine (*B–I*) and large intestine (*J–Q*) in mice expressing HAI-1 (*B–E* and *J–M*) and HAI-1-deficient mice (*F–I* and *N–Q*). Matriptase and E-cadherin is merged in *D*, *H*, *L*, and *P* with enlargements of the indicated area (shown with *white dotted line*) in *E*, *I*, *M*, and *Q*, respectively. Scale bar in *B*, 20 μm, representative for *B–D*, *F–H*, *J–L*, *N–P*. Scale bar in *E*, 5 μm, representative for *E*, *I*, *M*, and *Q*. The data are representative of two similar experiments.

C–F) and large (example in Fig. 4, *O–R*, compare with *K–N*) intestine, which were also observed in the control mice. Taken together, these findings suggest that endogenous HAI-2 is an important regulator of endogenous matriptase expression in intestinal epithelium.

Reduced HAI-2 Expression Enhances Matriptase Activation and Shedding in Epithelial Cell Monolayers—To mechanistically dissect the function of HAI-2 in polarized epithelium, we next silenced HAI-2 in intestinal epithelial Caco-2 cells (48) and studied the effect on matriptase expression. These cells were chosen because of their intestinal epithelial origin, because they express matriptase, prostasin, and HAI-2, and because they form matriptase and prostasin-dependent tight junctions with well-defined apical and basolateral membrane domains when cultured to confluency (33, 42, 49). Furthermore the Caco-2 cells allow easy detection of the various forms of matriptase in both lysates and conditioned media (Fig. 5*A*). Matriptase is synthesized as a 95 kDa protein that is processed in the SEA domain into the 70 kDa pro-form (zymogen). Upon activation, the 30 kDa serine protease domain of matriptase is cleaved but remains attached to the stem of the protease by disulfide bridges. The activated matriptase rapidly forms a 120 kDa complex with HAI-1 and is shed into the extracellular space in two different forms (Fig. 5*A*). HAI-2 expression was silenced using siRNA. To minimize the risk of off-target effects confounding data interpretation, we used three non-overlapping *SPINT2* siRNAs for silencing of HAI-2, as well as a combination of the three siRNAs for each experiment. All siRNA treatments resulted in a significant decrease in HAI-2 expression when compared with paired control siRNAs (example in Fig. 5*B*, *top panel*, *lanes 1–4*, compare with *lanes 5–8*). Similar to loss of HAI-2 in intestinal epithelium, silencing of HAI-2 in Caco-2 cells resulted in a dramatic decrease in cell-associated matriptase (example in Fig. 5*B*, *second panel from top*, *lanes 1–4*, compare with *5–8*). We found that only the 70 kDa pro-form of matriptase in the cell was reduced, while the activated form of matriptase (as represented in the 30-kDa form in the Western blot of reducing SDS/PAGE gels) was unaffected by the HAI-2 silencing. A marked reduction of cell-associated matriptase-HAI-1 complex was also observed by the HAI-2 silencing, as revealed by a 120-kDa species in SDS/PAGE and Western blot of non-boiled and non-reduced samples (example in Fig. 5*B*, *third panel from top*, *lanes 1–4*, compare with *lanes 5–8*). The level of prostasin was unaffected by the depletion of HAI-2 in the cell lysates (Fig. 5*B*, *second panel from bottom*, compare *lanes 1–4* to *5–8*). Importantly, the reduction of cell-associated matriptase, caused by HAI-2 silencing, was associated with a reciprocal increase in an activated soluble matriptase species shed into the conditioned medium. This was evidenced by large increases in activated matriptase, as represented in the 30-kDa form in the

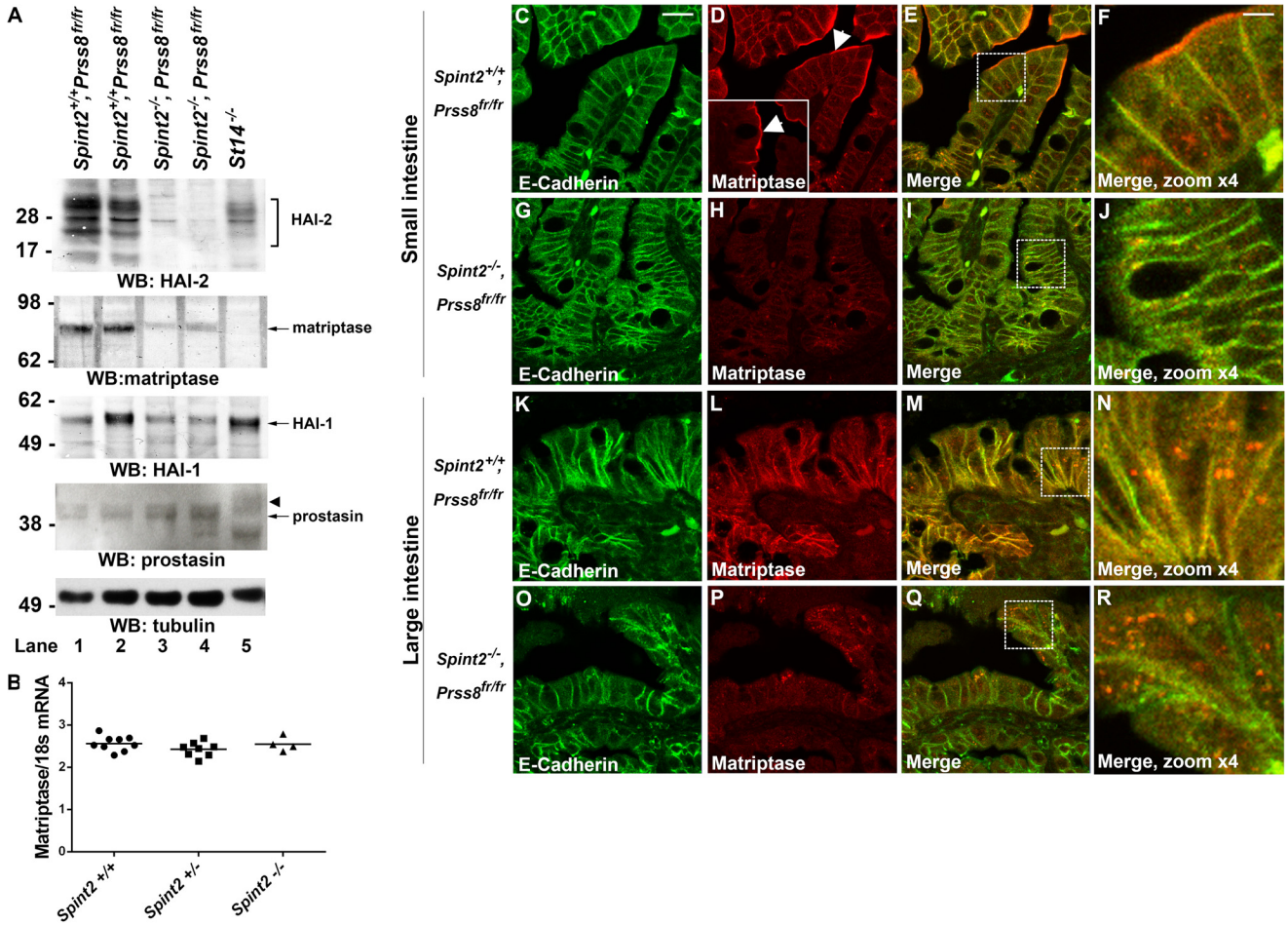

FIGURE 4. **Reduced expression of matriptase in HAI-2-deficient intestinal epithelium.** *A*, lysates of intestines from one-day-old HAI-2 expressing mice (*Spint2*$^{+/+}$; *Prss8*$^{fr/fr}$, *lanes 1* and *2*) and HAI-2-deficient littermates (*Spint2*$^{-/-}$;*Prss8*$^{fr/fr}$, *lanes 3* and *4*). Matriptase knock-out intestine (*St14*$^{-/-}$) from newborn mice was included as control (*lane 5*). The lysates were boiled, reduced and analyzed by SDS-PAGE and Western blot using antibodies against HAI-2 (*top panel*), matriptase (*second panel from top*), HAI-1 (*third panel from top*), and prostasin (*second panel from bottom*). The higher molecular forms of prostasin in matriptase knock-out tissue is marked with a *black arrowhead*. Tubulin was used as loading control (*bottom panel*). The specific proteins are indicated on the *right*, and molecular markers are indicated on the *left* (kDa). The data are representative of three similar experiments. *B*, mRNA was isolated from intestine from newborn *Spint2*$^{+/+}$($n = 9$), *Spint2* $^{+/-}$ ($n = 8$), and *Spint2*$^{-/-}$ ($n = 4$) mice, all in a prostasin hypomorphic background (*Prss8*$^{fr/fr}$). *St14* mRNA levels were analyzed by real-time PCR and are shown relative to 18 S ribosomal RNA. The distribution of matriptase (*D*, *H*, *L*, and *P*) and E-cadherin (*C*, *G*, *K*, and *O*) in small intestine (*C–J*) and large intestine (K-R) in mice expressing HAI-2 (*C–F* and *K–N*) and HAI-2-deficient mice (*G–J* and *O–R*). Unspecific matriptase staining, possibly from residual maternal milk in the intestine, (marked with a *white arrowhead* in *D*) is also observed in matriptase-deficient mice (*inset* in 4*D*, indicated with *white arrowhead*). Matriptase and E-cadherin are merged in *E*, *I*, *M*, and *Q* and enlargements of the area indicated with the *white dotted line* are shown in *F*, *J*, *N*, and *R*, respectively. Scale bar in $C = 20$ μm, is representative for *C–E*, *G–I*, *K—M*, and *O–Q*. Scale bar in $F = 5$ μm, is representative for *F*, *J*, *N*, and *R*. The data are representative of three similar experiments.

Western blot of reducing SDS/PAGE gels (example in Fig. 5*C*, *top panel*, *lanes 1–4*, compare with *lanes 5–8*) and in the 110 kDa soluble matriptase-HAI-1 complex revealed by SDS/PAGE and Western blot of non-boiled and non-reduced samples (example in Fig. 5*C*, *bottom panel*, *lanes 1–4*, compare with *lanes 5–8*). Taken together, this data shows that a reduction in HAI-2 levels results in a shift of matriptase from an immature, unprocessed cell-associated zymogen toward a mature, activated and inhibitor-complexed cell surface-shed form.

To further investigate the effect of HAI-2 levels on matriptase processing, we next performed immunofluorescence studies of confluent Caco-2 monolayers. We first validated the capacity of the mouse monoclonal matriptase antibody, M32, to specifically detect matriptase in this cell-based system. As shown in Fig. 6, strong staining of the basolateral plasma membrane was observed in Caco-2 monolayers treated with control siRNA (Fig. 6*F*), but not in Caco-2 monolayers treated with matriptase-silencing siRNA (Fig. 6*B*). As previously reported by us and by others, matriptase co-localized with occludin on the basolateral plasma membrane when the Caco-2 cells were transfected with a control siRNA (example in Fig. 6, *E–H*) (9, 42). However, as expected from the above biochemical analysis, matriptase expression was greatly diminished when HAI-2 was depleted using siRNA, with residual expression confined to intracellular vesicles and absence of plasma membrane co-localization with occludin (Fig. 6, *I–L*). We have previously reported that matriptase activation and HAI-1 complex formation is followed by endocytosis of this complex, which is consistent with the observations above (9).

Enhanced Matriptase Activation and Shedding Caused by Reduced HAI-2 Is Prostasin-dependent—To further investigate the role of HAI-2 in regulating matriptase post-translational processing, we used a previously established assay in which the activation of the matriptase target substrate, proteinase-acti-

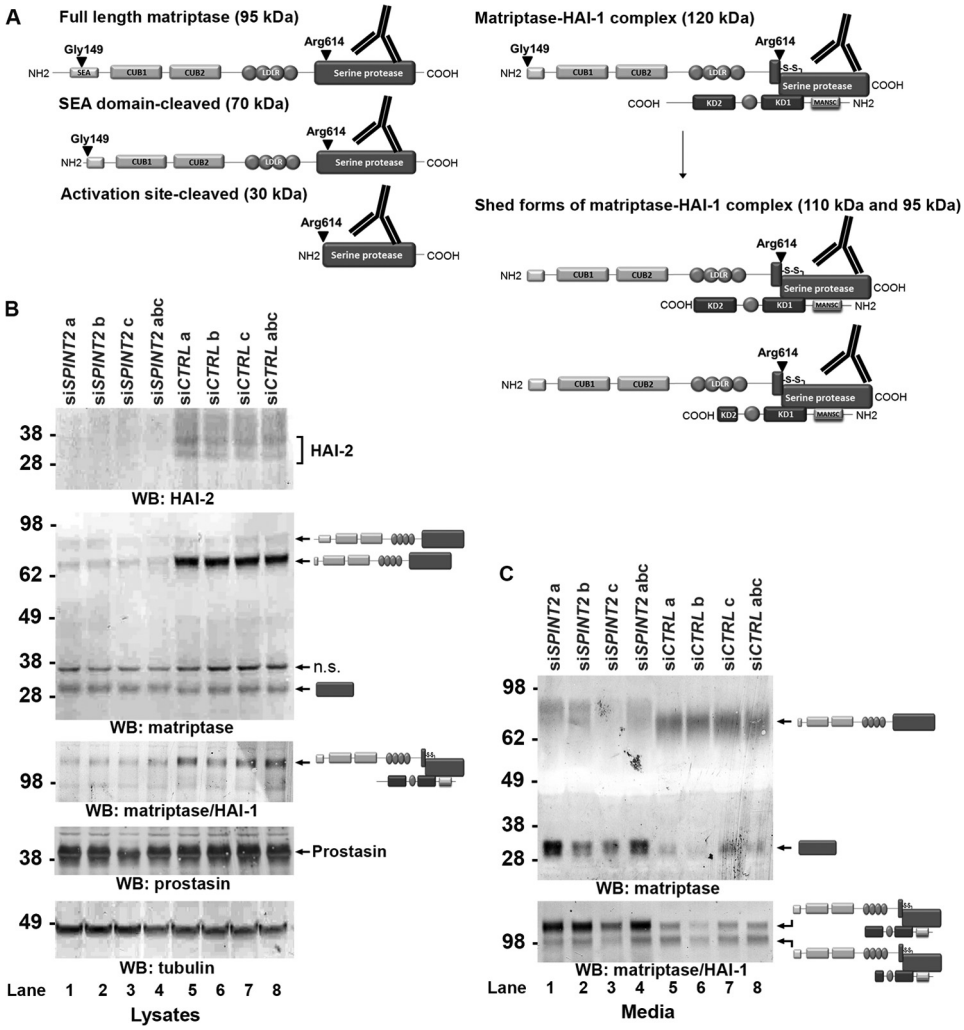

FIGURE 5. **Reduction of HAI-2 levels enhances matriptase activation and cell surface shedding in intestinal epithelial cell monolayers.** *A*, schematic depiction of full-length matriptase (*top*, *left*), SEA domain-cleaved matriptase (*left*, *middle*), activation site-cleaved matriptase (*left*, *bottom*), activated matriptase in complex with HAI-1 (*right*, *top*), and two forms of the matriptase-HAI-1 complex once shed from the cell surface (*right*, *middle*, and *bottom*). Positions of the SEA domain cleavage (Gly^{149}) and the activation cleavage site (Arg^{614}) are shown with *arrowheads*. The binding site for the antibody used to identify full-length, SEA domain-cleaved and activated matriptase by Western blot after reducing SDS-PAGE is indicated with a schematic drawing of an antibody (*left panel*). Also, the binding site for the antibody used to identify matriptase-HAI-1 complexes in the cell or as shed forms by Western blot under non-boiling/non-reducing conditions is indicated (*right panel*). *B* and *C*, three HAI-2-silencing siRNAs (si*SPINT2 a–c*, *lanes 1–4*) and three scrambled controls (si*CTRL a–c*, *lanes 5–8*) were transfected into Caco-2 cells. Three days post-transfection, the cell lysates (*B*) were analyzed by Western blot using antibodies against HAI-2 (*top panel*), matriptase (*second panel from top*), matriptase-HAI-1 complex formation (*third panel from top*, non-boiled/non-reduced) and prostasin (*second panel from bottom*). Tubulin was used as a loading control (*bottom panel*). Nonspecific bands are marked with *n.s.* *C*, conditioned medium from the cell samples from *B* was also analyzed using antibodies recognizing matriptase (*top panel*) and the matriptase-HAI-1 complex (*lower panel*). The specific proteins are indicated on the *right*, and the molecular markers are indicated on the *left* (kDa). The data are representative of five similar experiments.

vated receptor(PAR)-2 (4, 17, 51, 52), is measured by its ability to induce transcription of a serum response element(SRE)-luciferase reporter plasmid (16, 28). HEK293 cells, which express low levels of endogenous matriptase and prostasin, were transfected with a PAR-2 expression plasmid and with a doxycycline-inducible HAI-2 expression plasmid (Fig. 7*A*). As described recently (16), when these cells additionally were transfected with matriptase and prostasin expression plasmids, robust PAR-2 activation was observed, as shown by increased luciferase activity (Fig. 7*A*, *lane 1*). As expected, PAR-2 activation by the matriptase-prostasin complex was inhibited by induction of HAI-2 expression by doxycycline (Fig. 7*A*, *lane 2*). Transfection of HEK293 cells with matriptase or prostasin expression plasmids, individually in each case, resulted in a small, but significant, activation of PAR-2 (Fig. 7*A*, *lanes 3* and *5*, respectively). Interestingly, however, whereas induction of HAI-2 expression reduced prostasin-mediated PAR-2 activation to baseline levels (Fig. 7*A*, *lane 6*), the induction of HAI-2 did not significantly reduce PAR-2 activation by matriptase (Fig. 7*A*, *lane 4*). Compatible with a role of HAI-2 in regulating prostasin, an HA-tagged version of the inhibitor co-immunoprecipitated prostasin (Fig. 7*B*, *middle panels*) as well as matriptase, however mainly in its 95 kDa pro-form (Fig. 7*B*, *bottom panels*), in transfected HEK293 cells. Furthermore, endogenous prostasin was efficiently immunoprecipitated with HAI-2 antibodies in control siRNA-treated Caco-2 cells, but not from HAI-2-silenced Caco-2 cells (Fig. 7*C*, compare *lanes 1* and *4* with *3* and *6*).

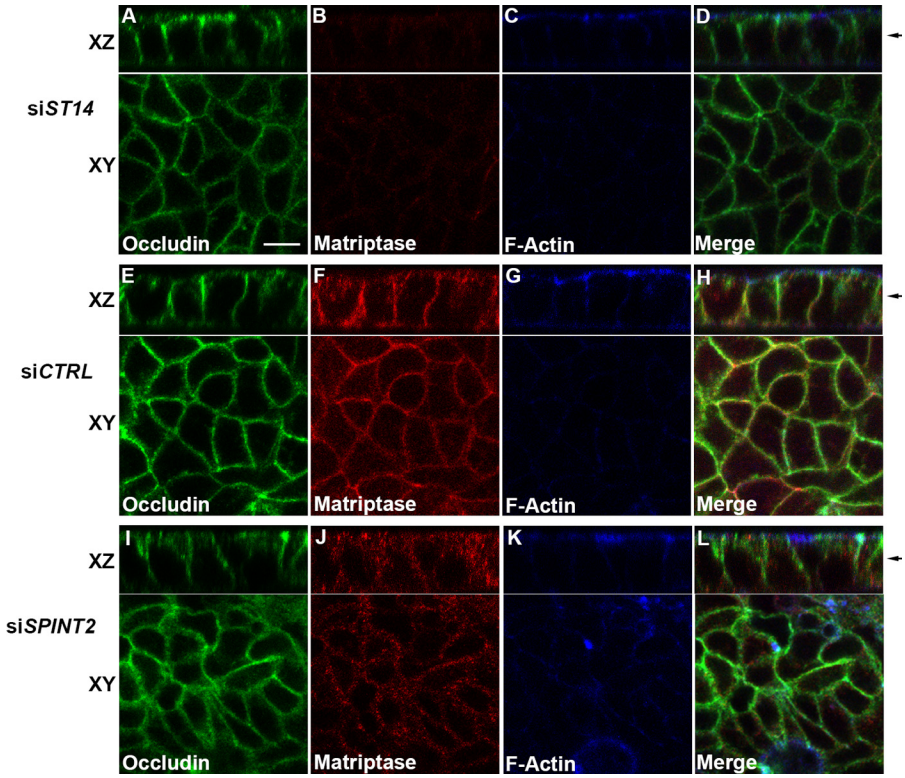

FIGURE 6. **Reduction of HAI-2 levels in intestinal epithelial cell monolayers reduces the expression and alters the subcellular localization of matriptase.** Caco-2 cells were transfected with matriptase siRNA (si*ST14*, *A–D*), control siRNA (si*CTRL*, *E–H*) or siRNA targeting HAI-2 (si*SPINT2*, *I–L*), and the cells were grown on transwell filters. Three days post-transfection, the siRNA transfected samples were fixed and co-stained with antibodies against occludin (*A*, *E*, *I*) and matriptase (*B*, *F*, *J*). Phalloidin was used as an apical marker to verify the polarization of the monolayer (*C*, *G*, *K*). All three stainings were merged in *D*, *H*, and *L*. Images were taken in the XY plane, showing a single section through the monolayer, and in the XZ plane, showing a cross-section of the monolayer using confocal imaging. The position of the XY section is indicated on the XZ section (*black arrows*) on the *right*. Scale bar, 10 μm. The data are representative of four similar experiments.

Taken together, these data tentatively suggest that HAI-2 may regulate the matriptase-prostasin complex by interacting with prostasin. A central prediction from this hypothesis would be that the "runaway" activation and consumptive depletion of matriptase from intestinal epithelial cells that was caused by reduced HAI-2 expression would be attenuated by the simultaneous reduction in the expression of prostasin. To challenge this hypothesis, we again used the Caco-2 cells and siRNA to determine if the simultaneous silencing of endogenous HAI-2 and prostasin would rescue the increased activation and shedding of matriptase observed by the single silencing of endogenous HAI-2. Two independent siRNAs were used to silence the expression of prostasin, both resulting in a significant reduction in the expression of the protease (example in Fig. 7*D*, *second panel from top*, compare *lanes 5–8* with *lanes 1–4*). As above, silencing of HAI-2 alone markedly reduced the levels of the 70-kDa proform of matriptase (Fig. 7*D*, *third panel from top*, compare *lanes 3* and *4* to *lanes 1* and *2*) and increased the shedding of the activated form to the conditioned medium, as detected by an increase in the 30-kDa matriptase serine protease domain (Fig. 7*E*, *top panel*, *lanes 3* and *4*, compare with *lanes 1* and *2*) and matriptase-HAI-1 complex formation (Fig. 7*E*, *bottom panel*, compare *lanes 3* and *4* to *lanes 1* and *2*). When prostasin levels were decreased, no variation in the total level of matriptase was observed both in the cell lysates (Fig. 7*D*, *third panel from top*, compare *lanes 5–8* with *lanes 1* and *2*) and in the conditioned medium (Fig. 7*E*, *top panel*, compare *lanes 5–8* with *1* and *2*), however, a slight reduction of matriptase-HAI-1 complex formation was observed both in the cell lysates (Fig. 7*D*, *second panel from bottom*, compare *lanes 5–8* to *lanes 1* and *2*) and in the conditioned medium (Fig. 7*E*, *bottom panel*, compare *lanes 5–8* to *lanes 1* and *2*). Interestingly, however, cells with simultaneous silencing of prostasin and HAI-2 displayed a markedly higher level of the 70-kDa matriptase proform than cells with silencing of HAI-2 alone (Fig. 7*D*, *third panel from top* and 7*E*, *top panel*, compare *lanes 9–12* with *lanes 3* and *4*). The decrease in matriptase-HAI-1 complex observed upon prostasin knock-down (Fig. 7*D*, *second panel from bottom*, *lanes 5–8* compare with *lanes 1* and *2*) was not rescued by the simultaneous knock-down of HAI-2 (Fig. 7*D*, *second panel from bottom*, *lanes 9–12*). To further characterize the rescue of matriptase expression levels by simultaneous depletion of both HAI-2 and prostasin, we next performed immunofluorescence studies of confluent Caco-2 monolayers. As described above, matriptase expression was greatly diminished when HAI-2 was depleted using siRNA (Fig. 7*J*). However, upon simultaneous depletion of prostasin (Fig. 7, *O–Q*), matriptase was once again observed on the basolateral plasma membrane, indistinguishable from the control cells (Fig. 7, *F–H*). Taken together, these data show that HAI-2 is an important regulator of matriptase that determines the rate of matriptase activation, matriptase-HAI-1 inhibitor complex formation, and matriptase shedding, by regulating the activity of prostasin.

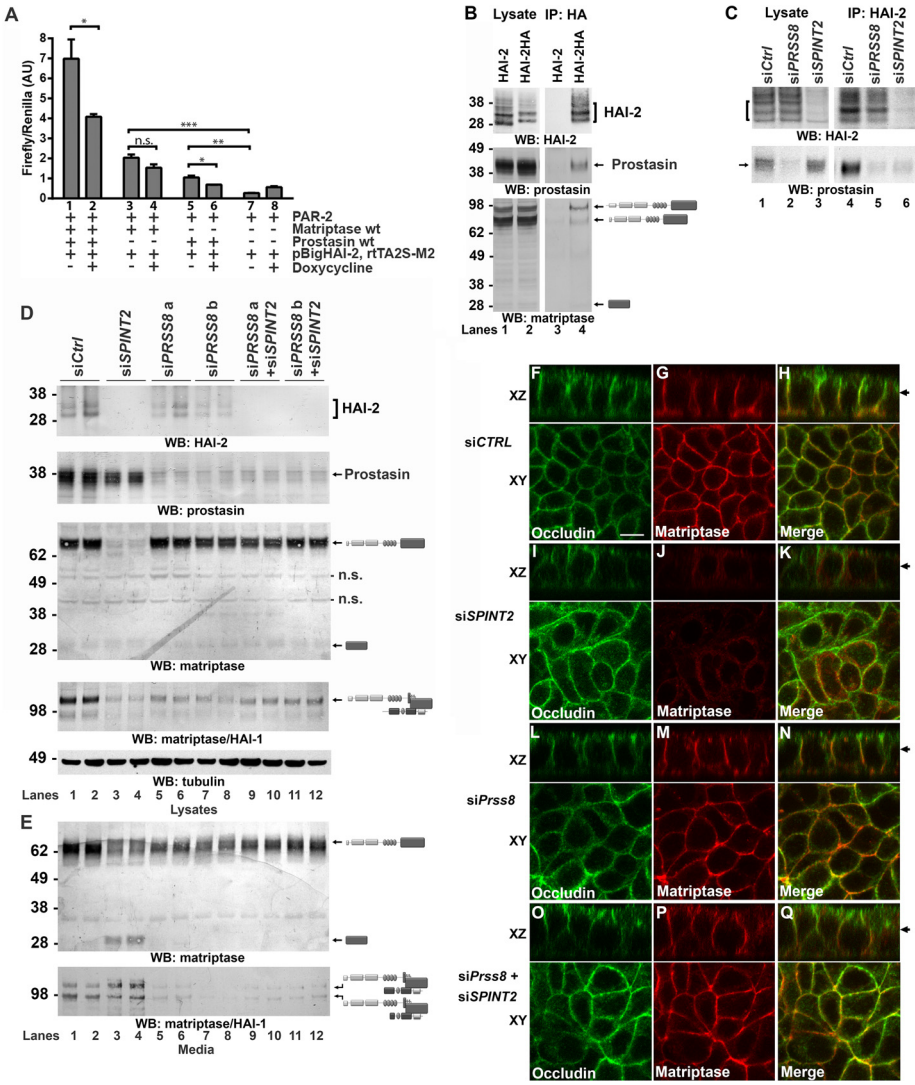

FIGURE 7. **Enhanced matriptase activation and shedding caused by reduction of HAI-2 levels is prostasin-dependent.** *A*, HEK293 cells were co-transfected with pSRE-firefly luciferase and pRL-Renilla luciferase reporter plasmids in combination with expression vectors for PAR-2 (*lanes 1–8*), matriptase (*lanes 1–4*), prostasin (*lanes 1–2* and *5–6*), and the doxycycline inducible rtTA2S-M2 tet-transactivator together with the pBigHAI-2 expression vector containing a tet-responsive element (*lanes 1–8*). Expression of HAI-2 was induced with doxycycline in *lanes 2*, *4*, *6*, and *8*. Data are shown as the mean ± S.D. of triplicate transfections of firefly luciferase units/*Renilla* luciferase units. *, $p < 0.05$; **, $p < 0.005$; ***, $p < 0.0005$, Student's *t* test, two-tailed. The data are representative of three similar experiments. *B*, HEK293T cells were co-transfected with matriptase (*lanes 1–4*), prostasin (*lanes 1–4*) and either HAI-2 (*lanes 1* and *3*) or HAI-2 containing an HA-tag (*lanes 2* and *4*). The cells were lysed 48 h after transfection and a fraction of the lysate (*lanes 1* and *2*) was analyzed by SDS-PAGE under reducing conditions followed by Western blot with HAI-2 (*top panel*), prostasin (*middle panel*), and matriptase (*bottom panel*) antibodies to verify the expression of the various proteins. The remaining lysate was used for immunoprecipitation (IP, *lanes 3* and *4*) with HA-antibodies and the precipitated proteins were subjected to SDS-PAGE and Western blot as for the lysates. HAI-2HA was successfully precipitated (*top panel*, *lane 4*) and prostasin efficiently co-precipitated with HAI-2HA (*middle panel*, *lane 4*). The 95 kDa pro-form of matriptase was also co-precipitated with HAI-2 HA (*bottom panel*, *lane 4*). The specific proteins are indicated on the *right*, and the molecular markers are indicated on the *left* (kDa). The data are representative of two similar experiments. *C*, Caco-2 cells were transfected with control siRNA (si*CTRL*, *lanes 1* and *4*), siRNA targeting prostasin (si*PRSS8*, *lanes 2* and *5*) or HAI-2 (si*SPINT2*, *lanes 3* and *6*). Three days post-transfection the cells were lysed and a fraction of the lysate (lysate, *lanes 1–3*) was analyzed by SDS-PAGE and Western blot using antibodies against HAI-2 (*top panel*) and prostasin (*bottom panel*). The remaining lysate was used for immunoprecipitation (IP, *lanes 4–6*) with HAI-2-antibodies and the precipitated proteins were subjected to SDS-PAGE and Western blot as for the lysates. Prostasin was efficiently co-precipitated with HAI-2. The specific proteins are indicated on the *right*, and the molecular markers are indicated on the *left* (kDa). The data are representative of two similar experiments. *D* and *E*, siRNAs for silencing down the gene of HAI-2 (si*SPINT2*, *lanes 3* and *4*), two prostasin-silencing siRNAs (si*Prss8* a and b, *lanes 5–8*) and a combination hereof (*lanes 9–12*) where transfected into Caco-2 cells. Scrambled siRNA was used as control (si*CTRL*, *lanes 1–2*). All samples were loaded in duplicates. *D*, three days post-transfection, the cell lysates were analyzed by Western blot using antibodies against HAI-2 (*top panel*), prostasin (*second panel from top*), matriptase (*third panel from top*), and the matriptase-HAI-1 complex (*second panel from bottom*, non-boiled/non-reduced). Tubulin was used as a loading control (*bottom panel*). *E*, conditioned media from the cell samples from *B* was also analyzed using an antibody recognizing matriptase (*top panel*) and the matriptase-HAI-1 complex (*bottom panel*). The specific proteins are indicated on the *right* and the molecular markers are indicated on the *left* (kDa). The data are representative of four similar experiments. *F–Q*, Caco-2 cells were transfected with scrambled siRNA as control (si*CTRL*, *F–H*) or siRNA against HAI-2 (si*SPINT2*, *I–K*), prostasin (si*PRSS8*, *L–N*), or both (si*PRSS8*+si*SPINT2*, *O-Q*). Three days post-transfection, the siRNA transfected samples were fixed and co-stained with antibodies against occludin (*F*, *I*, *L*, *O*) and matriptase (*G*, *J*, *M*, *Q*). The staining was merged in *H*, *K*, *N*, and *P*. Images were taken in the XY plane, showing a single section through the monolayer, and in the XZ plane showing a cross section of the monolayer using confocal imaging. The position of the XY section is indicated on the XZ section (*black arrows*) on the *right*. Scale bar, 10 μm. The data are representative of two similar experiments.

DISCUSSION

The current study directly examined the role of endogenous HAI-1 and HAI-2 in regulating endogenous matriptase trafficking and activation in polarized epithelium of the large and small intestine of mice. We found no evidence that loss of HAI-1 affected the abundance, steady state localization or state of activation of matriptase in either epithelium, suggesting that the primary function of HAI-1 in intestinal tissues, as regards matriptase, is to form inhibitor complexes with the activated protease. It should be noted that an independent study recently reported that ablation of HAI-1 from the mouse colon resulted in a diffuse cytoplasmic mislocalization of matriptase (36). Importantly, however, whereas we studied matriptase localization following the acute, tamoxifen-induced ablation of HAI-1 from the intestine, the matriptase localization studies in the aforementioned study were performed only after the overall demise of the intestinal epithelial architecture, caused by long-term HAI-1 ablation, was manifest (36), which may indirectly have affected the subcellular localization of matriptase.

The absence of an effect of HAI-1 on matriptase localization in intestinal epithelium *in vivo* is incongruent with cell-based overexpression studies in which both the efficient trafficking to the cell surface and the activation of overexpressed matriptase was shown to require the simultaneous overexpression of HAI-1 (see Introduction for references). While it is not within the scope of the current study to explain why these cell-based overexpression systems differ from polarized epithelium *in vivo* in terms of their requirement for regulation of matriptase by HAI-1, we speculate that supraphysiological levels of HAI-1 may be required to prevent pathogenic matriptase autoactivation within the secretory pathway caused by supraphysiological levels of expression of the protease.

In stark contrast to HAI-1, ablation of HAI-2 from intestinal epithelium of small and large intestine resulted in a near complete loss of matriptase from both epithelia. By using gene silencing in intestinal epithelial monolayers, we found that loss of HAI-2 markedly increased the activation and shedding of matriptase from the plasma membrane. The conspicuous absence of matriptase from HAI-2-ablated intestinal epithelium, therefore, likely can be attributed to the rate of activation and associated shedding of matriptase exceeding its rate of synthesis in the absence of HAI-2. This scenario is analogous to both consumptive coagulopathy and C1-inhibitor deficiency, where the uncontrolled activation of, respectively, coagulation- and complement system-associated serine proteases leads to a systemic depletion of their corresponding zymogens (54, 55). An important question emanating from our study is where in the secretory pathway HAI-2 acts to regulate prostasin-mediated matriptase activation? Currently available antibodies do not allow for specific detection of endogenous HAI-2 (data not shown). However, previous studies have shown that an epitope-tagged HAI-2 variant resides predominantly in an intracellular compartment when overexpressed in epithelial cells (33).

Our proposal that HAI-2 is essential for matriptase expression in intestinal epithelium by preventing the "consumptive depletion" of matriptase may also explain the etiology of the sodium-selective diarrhea that is associated with congenital HAI-2 deficiency in humans (56). The epithelial sodium channel ENaC is critical for sodium reabsorption in the distal colon, and the activity of ENaC in the distal colon is dependent on its proteolytic activation by the matriptase-prostasin system (53). It was, therefore, not intuitively obvious why HAI-2 deficiency is associated with decreased, rather than increased, sodium reabsorption. However, our model of HAI-2 deficiency-induced "consumptive depletion" of matriptase from colonic epithelium is fully compatible with this clinical manifestation of HAI-2-deficient individuals and is supported by a recent study that shows that HAI-2 can regulate prostasin-mediated ENaC activation (50).

Matriptase, prostasin, HAI-1, and HAI-2 are co-expressed in most developing and adult mammalian epithelia. It is important to underscore that the current study only provides evidence for how HAI-1 and HAI-2 regulate the matriptase-prostasin system in intestinal epithelium. Additional studies will be required to determine if similar regulation is observed in other simple, polarized epithelia, in transitional epithelium, and in multi-layered squamous epithelium.

Acknowledgments—We thank Drs. Silvio Gutkind and Mary Jo Danton for critically reviewing this manuscript.

REFERENCES

1. Szabo, R., and Bugge, T. H. (2011) Membrane anchored serine proteases in cell and developmental biology. *Annu. Rev. Cell Dev. Biol.* **27,** 213–235
2. Lin, C. Y., Anders, J., Johnson, M., Sang, Q. A., and Dickson, R. B. (1999) Molecular cloning of cDNA for matriptase, a matrix-degrading serine protease with trypsin-like activity. *J. Biol. Chem.* **274,** 18231–18236
3. Kim, M. G., Chen, C., Lyu, M. S., Cho, E. G., Park, D., Kozak, C., and Schwartz, R. H. (1999) Cloning and chromosomal mapping of a gene isolated from thymic stromal cells encoding a new mouse type II membrane serine protease, epithin, containing four LDL receptor modules and two CUB domains. *Immunogenetics* **49,** 420–428
4. Takeuchi, T., Harris, J. L., Huang, W., Yan, K. W., Coughlin, S. R., and Craik, C. S. (2000) Cellular localization of membrane-type serine protease 1 and identification of protease-activated receptor-2 and single-chain urokinase-type plasminogen activator as substrates. *J. Biol. Chem.* **275,** 26333–26342
5. Macao, B., Johansson, D. G., Hansson, G. C., and Härd, T. (2006) Autoproteolysis coupled to protein folding in the SEA domain of the membrane-bound MUC1 mucin. *Nat. Struct. Mol. Biol.* **13,** 71–76
6. Oberst, M. D., Williams, C. A., Dickson, R. B., Johnson, M. D., and Lin, C. Y. (2003) The activation of matriptase requires its noncatalytic domains, serine protease domain, and its cognate inhibitor. *J. Biol. Chem.* **278,** 26773–26779
7. Cho, E. G., Kim, M. G., Kim, C., Kim, S. R., Seong, I. S., Chung, C., Schwartz, R. H., and Park, D. (2001) N-terminal processing is essential for release of epithin, a mouse type II membrane serine protease. *J. Biol. Chem.* **276,** 44581–44589
8. Wang, J. K., Lee, M. S., Tseng, I. C., Chou, F. P., Chen, Y. W., Fulton, A., Lee, H. S., Chen, C. J., Johnson, M. D., and Lin, C. Y. (2009) Polarized epithelial cells secrete matriptase as a consequence of zymogen activation and HAI-1-mediated inhibition. *Am. J. Physiol. Cell Physiol.* **297,** C459–470
9. Friis, S., Godiksen, S., Bornholdt, J., Selzer-Plon, J., Rasmussen, H. B., Bugge, T. H., Lin, C. Y., and Vogel, L. K. (2011) Transport via the transcytotic pathway makes prostasin available as a substrate for matriptase. *J. Biol. Chem.* **286,** 5793–5802
10. Yu, J. X., Chao, L., and Chao, J. (1994) Prostasin is a novel human serine proteinase from seminal fluid. Purification, tissue distribution, and localization in prostate gland. *J. Biol. Chem.* **269,** 18843–18848

11. Yu, J. X., Chao, L., and Chao, J. (1995) Molecular cloning, tissue-specific expression, and cellular localization of human prostasin mRNA. *J. Biol. Chem.* **270,** 13483–13489
12. Shipway, A., Danahay, H., Williams, J. A., Tully, D. C., Backes, B. J., and Harris, J. L. (2004) Biochemical characterization of prostasin, a channel activating protease. *Biochem. Biophys. Res. Commun.* **324,** 953–963
13. Guo, J., Chen, S., Huang, C., Chen, L., Studholme, D. J., Zhao, S., and Yu, L. (2004) MANSC: a seven-cysteine-containing domain present in animal membrane and extracellular proteins. *Trends Biochem. Sci.* **29,** 172–174
14. Kawaguchi, T., Qin, L., Shimomura, T., Kondo, J., Matsumoto, K., Denda, K., and Kitamura, N. (1997) Purification and cloning of hepatocyte growth factor activator inhibitor type 2, a Kunitz-type serine protease inhibitor. *J. Biol. Chem.* **272,** 27558–27564
15. Shimomura, T., Denda, K., Kitamura, A., Kawaguchi, T., Kito, M., Kondo, J., Kagaya, S., Qin, L., Takata, H., Miyazawa, K., and Kitamura, N. (1997) Hepatocyte growth factor activator inhibitor, a novel Kunitz-type serine protease inhibitor. *J. Biol. Chem.* **272,** 6370–6376
16. Friis, S., Uzzun Sales, K., Godiksen, S., Peters, D. E., Lin, C. Y., Vogel, L. K., and Bugge, T. H. (2013) A matriptase-prostasin reciprocal zymogen activation complex with unique features: prostasin as a non-enzymatic co-factor for matriptase activation. *J. Biol. Chem.* **288,** 19028–19039
17. Camerer, E., Barker, A., Duong, D. N., Ganesan, R., Kataoka, H., Cornelissen, I., Darragh, M. R., Hussain, A., Zheng, Y. W., Srinivasan, Y., Brown, C., Xu, S. M., Regard, J. B., Lin, C. Y., Craik, C. S., Kirchhofer, D., and Coughlin, S. R. (2010) Local protease signaling contributes to neural tube closure in the mouse embryo. *Dev. Cell* **18,** 25–38
18. Netzel-Arnett, S., Currie, B. M., Szabo, R., Lin, C. Y., Chen, L. M., Chai, K. X., Antalis, T. M., Bugge, T. H., and List, K. (2006) Evidence for a matriptase-prostasin proteolytic cascade regulating terminal epidermal differentiation. *J. Biol. Chem.* **281,** 32941–32945
19. Lin, C. Y., Anders, J., Johnson, M., and Dickson, R. B. (1999) Purification and characterization of a complex containing matriptase and a Kunitz-type serine protease inhibitor from human milk. *J. Biol. Chem.* **274,** 18237–18242
20. Szabo, R., Hobson, J. P., List, K., Molinolo, A., Lin, C. Y., and Bugge, T. H. (2008) Potent inhibition and global co-localization implicate the transmembrane Kunitz-type serine protease inhibitor hepatocyte growth factor activator inhibitor-2 in the regulation of epithelial matriptase activity. *J. Biol. Chem.* **283,** 29495–29504
21. Lee, M. S., Kiyomiya, K., Benaud, C., Dickson, R. B., and Lin, C. Y. (2005) Simultaneous activation and hepatocyte growth factor activator inhibitor 1-mediated inhibition of matriptase induced at activation foci in human mammary epithelial cells. *Am. J. Physiol. Cell Physiol.* **288,** C932–941
22. Chen, Y. W., Wang, J. K., Chou, F. P., Chen, C. Y., Rorke, E. A., Chen, L. M., Chai, K. X., Eckert, R. L., Johnson, M. D., and Lin, C. Y. (2010) Regulation of the matriptase-prostasin cell surface proteolytic cascade by hepatocyte growth factor activator inhibitor-1 during epidermal differentiation. *J. Biol. Chem.* **285,** 31755–31762
23. Fan, B., Wu, T. D., Li, W., and Kirchhofer, D. (2005) Identification of hepatocyte growth factor activator inhibitor-1B as a potential physiological inhibitor of prostasin. *J. Biol. Chem.* **280,** 34513–34520
24. Carney, T. J., von der Hardt, S., Sonntag, C., Amsterdam, A., Topczewski, J., Hopkins, N., and Hammerschmidt, M. (2007) Inactivation of serine protease Matriptase1a by its inhibitor Hai1 is required for epithelial integrity of the zebrafish epidermis. *Development* **134,** 3461–3471
25. Szabo, R., Hobson, J. P., Christoph, K., Kosa, P., List, K., and Bugge, T. H. (2009) Regulation of cell surface protease matriptase by HAI2 is essential for placental development, neural tube closure and embryonic survival in mice. *Development* **136,** 2653–2663
26. Szabo, R., Molinolo, A., List, K., and Bugge, T. H. (2007) Matriptase inhibition by hepatocyte growth factor activator inhibitor-1 is essential for placental development. *Oncogene* **26,** 1546–1556
27. Szabo, R., Kosa, P., List, K., and Bugge, T. H. (2009) Loss of matriptase suppression underlies spint1 mutation-associated ichthyosis and postnatal lethality. *Am. J. Pathol.* **174,** 2015–2022
28. Szabo, R., Uzzun Sales, K., Kosa, P., Shylo, N. A., Godiksen, S., Hansen, K. K., Friis, S., Gutkind, J. S., Vogel, L. K., Hummler, E., Camerer, E., and Bugge, T. H. (2012) Reduced prostasin (CAP1/PRSS8) activity eliminates HAI-1 and HAI-2 deficiency-associated developmental defects by preventing matriptase activation. *PLoS Genet.* **8,** e1002937
29. Oberst, M. D., Chen, L. Y., Kiyomiya, K., Williams, C. A., Lee, M. S., Johnson, M. D., Dickson, R. B., and Lin, C. Y. (2005) HAI-1 regulates activation and expression of matriptase, a membrane-bound serine protease. *Am. J. Physiol. Cell Physiol.* **289,** C462–470
30. Tsuzuki, S., Murai, N., Miyake, Y., Inouye, K., Hirayasu, H., Iwanaga, T., and Fushiki, T. (2005) Evidence for the occurrence of membrane-type serine protease 1/matriptase on the basolateral sides of enterocytes. *Biochem. J.* **388,** 679–687
31. Miyake, Y., Tsuzuki, S., Yasumoto, M., Fushiki, T., and Inouye, K. (2009) Requirement of the activity of hepatocyte growth factor activator inhibitor type 1 for the extracellular appearance of a transmembrane serine protease matriptase in monkey kidney COS-1 cells. *Cytotechnology* **60,** 95–103
32. Miyake, Y., Yasumoto, M., Tsuzuki, S., Fushiki, T., and Inouye, K. (2009) Activation of a membrane-bound serine protease matriptase on the cell surface. *J. Biochem.* **146,** 273–282
33. Larsen, B. R., Steffensen, S. D., Nielsen, N. V., Friis, S., Godiksen, S., Bornholdt, J., Soendergaard, C., Nonboe, A. W., Andersen, M. N., Poulsen, S. S., Szabo, R., Bugge, T. H., Lin, C. Y., Skovbjerg, H., Jensen, J. K., and Vogel, L. K. (2013) Hepatocyte growth factor activator inhibitor-2 prevents shedding of matriptase. *Exp. Cell Res.* **319,** 918–929
34. Miyake, Y., Tsuzuki, S., Fushiki, T., and Inouye, K. (2010) Matriptase does not require hepatocyte growth factor activator inhibitor type-1 for activation in an epithelial cell expression model. *Biosci. Biotechnol. Biochem.* **74,** 848–850
35. Kilpatrick, L. M., Harris, R. L., Owen, K. A., Bass, R., Ghorayeb, C., Bar-Or, A., and Ellis, V. (2006) Initiation of plasminogen activation on the surface of monocytes expressing the type II transmembrane serine protease matriptase. *Blood* **108,** 2616–2623
36. Kawaguchi, M., Takeda, N., Hoshiko, S., Yorita, K., Baba, T., Sawaguchi, A., Nezu, Y., Yoshikawa, T., Fukushima, T., and Kataoka, H. (2011) Membrane-bound serine protease inhibitor HAI-1 is required for maintenance of intestinal epithelial integrity. *Am. J. Pathol.* **179,** 1815–1826
37. List, K., Haudenschild, C. C., Szabo, R., Chen, W., Wahl, S. M., Swaim, W., Engelholm, L. H., Behrendt, N., and Bugge, T. H. (2002) Matriptase/MT-SP1 is required for postnatal survival, epidermal barrier function, hair follicle development, and thymic homeostasis. *Oncogene* **21,** 3765–3779
38. Kosa, P., Szabo, R., Molinolo, A. A., and Bugge, T. H. (2012) Suppression of Tumorigenicity-14, encoding matriptase, is a critical suppressor of colitis and colitis-associated colon carcinogenesis. *Oncogene* **31,** 3679–3695
39. Lin, C. Y., Wang, J. K., Torri, J., Dou, L., Sang, Q. A., and Dickson, R. B. (1997) Characterization of a novel, membrane-bound, 80-kDa matrix-degrading protease from human breast cancer cells. Monoclonal antibody production, isolation, and localization. *J. Biol. Chem.* **272,** 9147–9152
40. Alam, J., and Cook, J. L. (1990) Reporter genes: application to the study of mammalian gene transcription. *Anal. Biochem.* **188,** 245–254
41. Katsantoni, E. Z., Anghelescu, N. E., Rottier, R., Moerland, M., Antoniou, M., de Crom, R., Grosveld, F., and Strouboulis, J. (2007) Ubiquitous expression of the rtTA2S-M2 inducible system in transgenic mice driven by the human hnRNPA2B1/CBX3 CpG island. *BMC Dev. Biol.* **7,** 108
42. Buzza, M. S., Netzel-Arnett, S., Shea-Donohue, T., Zhao, A., Lin, C. Y., List, K., Szabo, R., Fasano, A., Bugge, T. H., and Antalis, T. M. (2010) Membrane-anchored serine protease matriptase regulates epithelial barrier formation and permeability in the intestine. *Proc. Natl. Acad. Sci. U.S.A.* **107,** 4200–4205
43. List, K., Kosa, P., Szabo, R., Bey, A. L., Wang, C. B., Molinolo, A., and Bugge, T. H. (2009) Epithelial integrity is maintained by a matriptase-dependent proteolytic pathway. *Am. J. Pathol.* **175,** 1453–1463
44. List, K., Szabo, R., Molinolo, A., Nielsen, B. S., and Bugge, T. H. (2006) Delineation of matriptase protein expression by enzymatic gene trapping suggests diverging roles in barrier function, hair formation, and squamous cell carcinogenesis. *Am. J. Pathol.* **168,** 1513–1525
45. Itoh, H., Kataoka, H., Hamasuna, R., Kitamura, N., and Koono, M. (1999) Hepatocyte growth factor activator inhibitor type 2 lacking the first Kunitz-type serine proteinase inhibitor domain is a predominant product in mouse but not in human. *Biochem. Biophys. Res. Commun.* **255,** 740–748

46. Xu, H., Xu, Z., Tseng, I. C., Chou, F. P., Chen, Y. W., Wang, J. K., Johnson, M. D., Kataoka, H., and Lin, C. Y. (2012) Mechanisms for the control of matriptase activity in the absence of sufficient HAI-1. *Am. J. Physiol. Cell Physiol.* **302,** C453–462
47. Spacek, D. V., Perez, A. F., Ferranti, K. M., Wu, L. K., Moy, D. M., Magnan, D. R., and King, T. R. (2010) The mouse frizzy (fr) and rat 'hairless' (frCR) mutations are natural variants of protease serine S1 family member 8 (Prss8). *Exp. Dermatol.* **19,** 527–532
48. Fogh, J., and Trempe, G. (1975) *Human Tumor Cells in Vitro* (Fogh, J., ed) pp. 115–141, Plenum Press, New York, NY
49. Buzza, M. S., Martin, E. W., Driesbaugh, K. H., Désilets, A., Leduc, R., and Antalis, T. M. (2013) Prostasin is required for matriptase activation in intestinal epithelial cells to regulate closure of the paracellular pathway. *J. Biol. Chem.* **288,** 10328–10337
50. Faller, N., Gautschi, I., and Schild, L. (2014) Functional Analysis of a Missense Mutation in the Serine Protease Inhibitor SPINT2 Associated with Congenital Sodium Diarrhea. *PLoS One* **9,** e94267
51. Nystedt, S., Emilsson, K., Wahlestedt, C., and Sundelin, J. (1994) Molecular cloning of a potential proteinase activated receptor. *Proc. Natl. Acad. Sci. U.S.A.* **91,** 9208–9212
52. Sales, K. U., Friis, S., Konkel, J. E., Godiksen, S., Hatakeyama, M., Hansen, K. K., Rogatto, S. R., Szabo, R., Vogel, L. K., Chen, W., Gutkind, J. S., and Bugge, T. H. (2014) Non-hematopoietic PAR-2 is essential for matriptase-driven pre-malignant progression and potentiation of ras-mediated squamous cell carcinogenesis. *Oncogene* 10.1038/onc.2013.563
53. Malsure, S., Wang, Q., Charles, R. P., Sergi, C., Perrier, R., Christensen, B. M., Maillard, M., Rossier, B. C., and Hummler, E. (2014) Colon-Specific Deletion of Epithelial Sodium Channel Causes Sodium Loss and Aldosterone Resistance. *J. Am. Soc. Nephrol.* 10.1681/ASN.2013090936
54. Davis, A. E., 3rd. (2005) The pathophysiology of hereditary angioedema. *Clin. Immunol.* **114,** 3–9
55. Colman, R. W., Robboy, S. J., and Minna, J. D. (1979) Disseminated intravascular coagulation: a reappraisal. *Annu. Rev. Med.* **30,** 359–374
56. Heinz-Erian, P., Müller, T., Krabichler, B., Schranz, M., Becker, C., Rüschendorf, F., Nürnberg, P., Rossier, B., Vujic, M., Booth, I. W., Holmberg, C., Wijmenga, C., Grigelioniene, G., Kneepkens, C. M., Rosipal, S., Mistrik, M., Kappler, M., Michaud, L., Dóczy, L. C., Siu, V. M., Krantz, M., Zoller, H., Utermann, G., and Janecke, A. R. (2009) Mutations in SPINT2 Cause a Syndromic Form of Congenital Sodium Diarrhea. *Am. J. Hum. Genet.* **84,** 188–196